Development of multi-scale modeling software for entangled soft matter in advanced soldier protection

Investigators:

Jay D. Schieber (Professor, PI), David Venerus (Professor, co-PI),
Department of Chemical and Biological Engineering
Illinois Institute of Technology
10 W. 33rd Street
Chicago, Illinois 60616
Telephone: (312) 567-3046
Fax: (312) 567-8874
email: schieber@iit.edu, venerus@iit.edu, perezluna@iit.edu

and

H. Larry Scott (Professor, co-PI)
Department of Physics
Illinois Institute of Technology
3101 South Dearborn St
Chicago, Illinois 60616
Telephone: (312) 567-3480
Fax: 312.567.3494
email: scotth@iit.edu, gidalevitz@iit.edu, orgel@iit.edu

Final report, December 6, 2011

20120117032

DTIC® has determined on 2 / 9 2012 that this Technical Document has the Distribution Statement checked below. The current distribution for this document can be found in the DTIC® Technical Report Database.

☒ **DISTRIBUTION STATEMENT A.** Approved for public release; distribution is unlimited.

☐ **© COPYRIGHTED.** U.S. Government or Federal Rights License. All other rights and uses except those permitted by copyright law are reserved by the copyright owner.

☐ **DISTRIBUTION STATEMENT B.** Distribution authorized to U.S. Government agencies only (fill in reason) (date of determination). Other requests for this document shall be referred to (insert controlling DoD office).

☐ **DISTRIBUTION STATEMENT C.** Distribution authorized to U.S. Government Agencies and their contractors (fill in reason) (date determination). Other requests for this document shall be referred to (insert controlling DoD office).

☐ **DISTRIBUTION STATEMENT D.** Distribution authorized to the Department of Defense and U.S. DoD contractors only (fill in reason) (date of determination). Other requests shall be referred to (insert controlling DoD office).

☐ **DISTRIBUTION STATEMENT E.** Distribution authorized to DoD Components only (fill in reason) (date of determination). Other requests shall be referred to (insert controlling DoD office).

☐ **DISTRIBUTION STATEMENT F.** Further dissemination only as directed by (insert controlling DoD office) (date of determination) or higher DoD authority.

Distribution Statement F is also used when a document does not contain a distribution statement and no distribution statement can be determined.

☐ **DISTRIBUTION STATEMENT X.** Distribution authorized to U.S. Government Agencies and private individuals or enterprises eligible to obtain export-controlled technical data in accordance with DoDD 5230.25; (date of determination). DoD Controlling Office is (insert controlling DoD office).

January 5, 2012

Via email:

Jan Andzelm, Cooperative Agreement Manager	email: jandzelm@us.army.mil
Kevin Bassler, Agreement Administration Officer	email: kevin.bassler@us.army.mil
Julia Wertley-Rotenberry , Grants Officer	email: julia.wertleyrotenberry@us.army.mil

Via hard copy:

Defense Technical Information Center (DTIC)
8725 John J. Kingman Road, Suite 0944
Ft. Belvoir, VA 22060-6218

RE: W911NF-08-2-0058 Final report
       Dr. Jay Schieber, Illinois Institute of Technology, (OSRP# 6186)

The Illinois Institute of Technology is pleased to provide you with this report as referenced above.

If you should have any technical questions, please contact Dr. Schieber at 312-567-3046 or via email at schieber@iit.edu. If you should have any administrative questions, please do not hesitate to contact me at 312-567-3035 or via email at pappas@iit.edu.

Sincerely,

Domenica G. Pappas, CRA
Director
Sponsored Research and Programs

cc: Jay Schieber, Ph.D. (via email: schieber@iit.edu)
       Office of Naval Research, Thomas Pettit (via email: thomas.pettit@navy.mil), cover letter only

Contents

List of Figures

1 Statement of the problem studied

The Department of Defense seeks to develop body armor that is, among other things, lighter and more flexible. For example, the new armor based on shear thickening fluids (STF) is very

flexible, but stiffens under the load of impacting projectiles in order to provide protection. Hence, the interaction of the armor with human tissue (e.g., muscle) becomes very important. However, there is not sufficient understanding in how tissue responds to the large stresses, and high strain rates that occur in such interactions. Moreover, in order to test armor candidates, one needs a synthetic material that can mimic the response of tissue. Our projects seek to address both of these limitations, both by modeling the transient mechanical (rheological) properties of tissue, and by developing software that can predict the same response of many possible synthetic testing materials.

Specifically, we proposed the following:

1. Generalization of our entanglement theory to cross-linked systems.

2. A progressive coarse graining of the theory to create a continuum-level description. Success here would create a model more amenable to simulation in complex geometries. This was a longer-term goal, with no promised deliverables in the time frame of the proposal.

3. Make available to the Army resulting computer code.

4. Generalization to co-polymers.

5. Generalization to semi-flexible polymers. Such polymers are ubiquitous in tissue, and largely determine their rheological and mechanical properties.

We will summarize achievements and deliverables for each of these points below.

2 Summary of the most important results

2.1 Generalization of our entanglement theory to cross-linked systems.

The Multifunctional Materials Branch (MMB) of the Army Research Laboratory (ARL) has been developing cross-linked polymer gels as candidate materials to mimic human tissue. Such a mimetic is necessary to develop certification protocols for proposed advanced body armor. To be successful these materials should mimic tissue's rheological and mechanical response. The possible parameter space for such material is very large, so a guiding theoretical framework is necessary to focus synthetic and experimental efforts.

The slip-link model, in particular its discrete version (DSM) has shown great success at describing the rheological material of linear, monodisperse entangled polymers, without parameter adjustment. It is based on statistical mechanics, and has strong connections to non-equilibrium thermodynamics. Moreover, it is substantially robust, so able to handle virtually all flow fields, polymer architectures and blends of polymers, without change to the mathematical structure. Basically, one needs only to perform some statistical mechanical calculations for chain architecture (including semi-flexibility) as input to the structure.

2

In order to apply this theory to the problem at hand—predicting the rheology of cross-linked gels with entangled, structured solvents, we needed to solve several theoretical and practical problems to make the numerical calculations sufficiently robust. First, the implementation had to include blends of polymers. The theory is a single-chain, mean-field object so that blending effects occur through entanglement dynamics. Calculations are performed via ensemble averages of simulation trajectories, whose algorithms were rigorously derived from the proposed evolution equation. However, in order to be computationally efficient, it was important to keep all dynamics local to individual trajectories in the ensemble. Hence, we continued to utilize an entanglement survival function, but generalized it to blends. This is conceptually straightforward, but created a few practical obstacles. Once our solutions were implemented, we were able to show that the theory could indeed make quantitative predictions of the rheology of blends. These results were published in *Macromolecules*, as detailed below. Another manuscript also examining simultaneous dielectric relaxation of monodisperse, bidisperse, and star-branched entangled polymers will also be submitted for publication very soon.

We were then able to implement the theory to model the rheology of cross-linked systems. However, the theory also requires as input the cross-linked structure that arises during curing or cross-linking of the gel. Such structure should come from other models. However, to avoid ambiguity in the tests of the theory, we considered monodisperse, end-functionalized chains. These networks are somewhat idealized, but obtainable experimentally. Here, comparison with theory allowed us to interpret and clarify important physics in cross-linked systems. These results were published in *Rheologica Acta*, as discussed below.

2.1.1 Bidisperse blends of linear polymers

The following description of the theory is taken from [9]. The chain is approximated by a random walk. The entanglements are randomly distributed along the chain with uniform probability $1/(1+\beta)$, defining the primitive-path of the chain, where β is a model parameter that is defined below. It is assumed that relaxation of an entangled strand is much faster then the chain relaxation, so the chain may be coarse-grained to a primitive-path. The model is described by the following variables: the number of strands, Z, in a chain; the number of Kuhn steps, N_i, in the ith strand; the vector, $\boldsymbol{Q}_i$, connecting entanglements $i-1$ and i; and the characteristic life-time, τ_i^{CD}, of the ith entanglement related to constraint dynamics (CD). The equilibrium probability density, $p_{\text{eq},\gamma}(\Omega)$, of conformations of a type γ chain, which denotes chain length, is given by the modified Maxwell-Boltzmann relationship

$$p_{\text{eq},\gamma}(\Omega) = \frac{\delta\left(N_{\text{K},\gamma}, \sum_{i=1}^{Z} N_i\right)}{J\beta^{Z-1}} \exp\left[-\frac{F(\Omega)}{k_{\text{B}}T}\right] \prod_{i=1}^{Z-1} p^{\text{CD}}(\tau_i^{\text{CD}}), \tag{1}$$

where $J = (1+1/\beta)^{N_{\text{K}}-1}$ is the normalization constant, $\delta(i,j)$ is the Kronecker delta function, $N_{\text{K},\gamma}$ is the total number of Kuhn steps in a chain of type γ, $F(\Omega)$ is the free energy of a chain with conformation Ω, T is temperature, $p^{\text{CD}}(\tau^{\text{CD}})$ is the probability density of

3

entanglement life-times, k_B is the Boltzmann constant, and β is a parameter that depends on entanglement density and approximately equal to $N_e - 1$ for long chains, where $N_e \equiv \langle N_i \rangle$ is the average number of Kuhn steps in a strand [10].

Here, the free energy of an entangled strand is approximated by the Gaussian free energy [21]

$$\frac{F_s(\boldsymbol{Q}, N)}{k_B T} = \frac{3Q^2}{2Na_K^2} + \frac{3}{2}\ln\left[\frac{2\pi N}{3a_K^2}\right].$$ (2)

The approximation is valid for flexible polymer chains that are not stretched greater than about 1/3 of their contour length. The free energy of the dangling ends is found to be zero, so the free energy of the entire chain is

$$F(\Omega) = \sum_{i=2}^{Z-1} F_s(\boldsymbol{Q}_i, N_i).$$ (3)

In DSM N_i is treated as an integer number, so conformation changes due to Brownian forces are described by a jump process from one conformation to another. The evolution equation at equilibrium becomes

$$\frac{\partial p_{\mathrm{eq},\gamma}(\Omega, t|\Omega_0, t_0)}{\partial t} = \int \left[W(\Omega|\Omega') p_{\mathrm{eq},\gamma}(\Omega', t|\Omega_0, t_0) - W(\Omega'|\Omega) p_{\mathrm{eq},\gamma}(\Omega, t|\Omega_0, t_0) \right] d\Omega',$$ (4)

where $W(\Omega'|\Omega)$ is a transition rate probability of a jump from conformation Ω to Ω' in unit time. τ_K is a characteristic time required to shift one Kuhn step through an entanglement, which depends on the polymer chemistry and temperature, but not the polymer architecture nor molecular weight. Note that jumps to conformation Ω are allowed only from a neighboring conformation Ω', so $W(\Omega|\Omega')$ can be split into five processes

$$W = \left(\sum_{i=1}^{Z-1} W_{\mathrm{sh}}^i \right) + W_d^{\mathrm{SD}} + W_c^{\mathrm{SD}} + W_d^{\mathrm{CD}} + W_c^{\mathrm{CD}},$$ (5)

where W_{sh}^i is a transition probability per time to shift a Kuhn step through entanglement i, W_d^{SD} and W_c^{SD} are related to probabilities to destroy and create an entanglement on the ends of the chain by SD, and W_d^{CD} and W_c^{CD} are transition probabilities per time to destroy and create an entanglement in the middle of the chain by CD. Complete expressions for the transition probabilities are reported in reference [10], but we give an example here. The transition probability to shift a Kuhn step between strands i and $i+1$ is

$$
\begin{aligned}
W_{\mathrm{sh}}^i(\Omega'|\Omega) = {} & \delta_{Z,Z'} \prod_{j=2}^{Z-1} \delta\left(\boldsymbol{Q}_j - \boldsymbol{Q}_j'\right) \sum_{j=1}^{Z-1} \delta\left(\tau_j^{\mathrm{CD}} - \tau_j^{\mathrm{CD}'}\right) \prod_{j=1, j \neq i, i+1}^{Z} \delta_{N_j, N_j'} \times \\
& \left(\delta_{N_i, N_i'-1} \delta_{N_{i+1}, N_{i+1}'+1} + \delta_{N_i, N_i'+1} \delta_{N_{i+1}, N_{i+1}'-1} \right) \times \\
& \frac{2(\beta+1)}{\tau_K(N_i + N_{i+1})} \exp\left[\frac{F(\Omega') - F(\Omega)}{2k_B T} \right],
\end{aligned}
$$ (6)

4

The first line in the equation preserves conformations of the strands that are not involved in the Kuhn step shuffling through entanglement i. The second line ensures that only one Kuhn step can be shuffled at a time through entanglement i. The last line shows that Kuhn step shuffling is a result of Brownian forces as well as free energy differences. τ_K is a time constant related to the friction coefficient of a single step in the chain, which depends only on the chemistry and temperature of the polymer (and solvent concentration, if present). In the present work, the total chain friction is assumed to be proportional to the number of Kuhn steps in the entire chain. Hence, the total friction of the chain is constant [16]. In addition, the transition probability satisfies detailed balance (sec.6 in reference [23]).

In DSM an entanglement is formed by at least two chains, so if one chain abandons an entanglement then it should be destroyed for the other chain(s). The simplest realization of such CD would be to couple several chains in the ensemble as was done by Doi and Takimoto [2]. However, such an implementation loses some advantages of a mean-field theory. To develop a self-consistent realization with independent chains in the ensemble we add a characteristic life-time, τ^{CD}, to each entanglement. The distribution of the life-times, $p^{CD}(\tau^{CD})$, will affect the rate of destruction of the entanglements by CD, which should be self-consistent with the rate of destruction by SD [10]. $p^{CD}(\tau^{CD})$ is defined by chain-chain interactions, so it depends on polydispersity and complexity of entanglements. We show how to calculate $p^{CD}(\tau^{CD})$ for a polydisperse blend with any average number of chains, α, entangled with the probe chain. We assume that any given entanglement consists of an integer number of chains, but on average the number can be non-integer. If α is non-integer, the simplest implementation is to allow only entanglements with the integer number of chains closest to α. Although, more realistic might be to use a Poisson distribution, we are interested here in sensitivity effects of entanglement complexity. $p^{CD}(\tau^{CD})$ is found in a self-consistent way from chain SD using the following equation

$$
p^{CD}(\tau^{CD}) = (\text{int}(\alpha) - \alpha) \underbrace{\int_0^\infty \ldots \int_0^\infty}_{\text{int}(\alpha)-1} \delta\left(\tau^{CD} - 1 \Big/ \sum_{i=1}^{\text{int}(\alpha)-1} \frac{1}{\tau_i}\right) \prod_{i=1}^{\text{int}(\alpha)-1} p^{SD}(\tau_i) d\tau_i +
$$

$$
(\alpha - \text{int}(\alpha) + 1) \underbrace{\int_0^\infty \ldots \int_0^\infty}_{\text{int}(\alpha)} \delta\left(\tau^{CD} - 1 \Big/ \sum_{i=1}^{\text{int}(\alpha)} \frac{1}{\tau_i}\right) \prod_{i=1}^{\text{int}(\alpha)} p^{SD}(\tau_i) d\tau_i, \quad (7)
$$

where $\text{int}(\alpha)$ is the smallest integer value that is equal to or greater than α. $p^{SD}(\tau)$ is obtained from the fraction of survived entanglements, $f^{SD}(t)$, that are being destroyed by SD only

$$
f^{SD}(t) = \int_0^\infty p^{SD}(\tau) \exp\left(-\frac{t}{\tau}\right) d\tau. \quad (8)
$$

For binary entanglements ($\alpha = 1$) eq.(7) becomes equivalent to that used in references [10, 14, 18]. We examined the sensitivity of prediction on the value of α, and discovered that only binary entanglements are consistent with data. Such a result is consistent with

the primitive path analysis results discussed below. As a result we will consider only binary entanglements from now on.

For a polydisperse blend of n_m components with volume fractions w_γ, $f^{\text{SD}}(t)$ is split into a fraction of survived entanglements of the individual components $f_\gamma^{\text{SD}}(t)$ as follows

$$f^{\text{SD}}(t) = \sum_{\gamma=1}^{n_m} w_\gamma f_\gamma^{\text{SD}}(t). \tag{9}$$

Note that for the blends considered in this paper, volume and weight fractions are assumed to be the same, so we choose to use weight fraction. However, in a more complicated blend, volume fraction would be more appropriate.

We assume that entanglement characteristic life-times are all independent, ignoring the fact that two chains once entangled have a higher chance to entangle again, so $p^{\text{CD}}(\tau^{\text{CD}})$ is not affected by neighboring values of τ^{CD}. Assuming binary interactions and using eq. 7 and eq. 9, $p^{\text{CD}}(\tau^{\text{CD}})$ is constructed from life-time distributions of its monodisperse components

$$p^{\text{CD}}(\tau^{\text{CD}}) = \sum_{\gamma=1}^{n_m} w_\gamma p_\gamma^{\text{CD}}(\tau^{\text{CD}}), \tag{10}$$

where $p_\gamma^{\text{CD}}(\tau^{\text{CD}})$ is the entanglement characteristic life-time distribution for the γth component. The details on how $p_\gamma^{\text{CD}}(\tau^{\text{CD}})$ is estimated for a monodisperse component are given in reference [10], and has the following form

$$p_\gamma^{\text{CD}}(\tau) = \frac{(1-g_\gamma)\alpha_\gamma}{\left(\tau_\gamma^{\text{max}}\right)^{\alpha_\gamma} - \left(\tau_\gamma^0\right)^{\alpha_\gamma}} \tau^{\alpha_\gamma-1} H(\tau - \tau_\gamma^0) H(\tau_\gamma^{\text{max}} - \tau) - g_\gamma \delta(\tau_\gamma^{\text{d}} - \tau), \tag{11}$$

where g_γ, α_γ, τ_γ^0, τ_γ^{max}, τ_γ^{d} are parameters determined self-consistently by τ_{K}, $N_{\text{K},\gamma}$ and β. $H(x)$ is the Heaviside step function. The first term is a result of CLF and the second term is related to reptation [10].

After calculating $p^{\text{CD}}(\tau^{\text{CD}})$ and using it in eq. 1 we predict the relaxation modulus of the blend, $G(t)$

$$G(t) = \frac{1}{nk_{\text{B}}T} \langle \tau_{xy}(0)\tau_{xy}(t)\rangle_{\text{eq}}, \tag{12}$$

where $\langle \cdots \rangle_{\text{eq}}$ is an ensemble average, $n = \sum_\gamma n_\gamma = \rho N_{\text{A}} \sum_\gamma (w_\gamma/M_{\text{w},\gamma})$ is the number density of polymer chains, n_γ is the number density of type γ polymer chains, ρ is the polymer density (assumed here to be independent of polymer molecular-weight), N_{A} is the Avogadro constant, and $\tau_{xy}(t)$ is any off-diagonal stress tensor component. Note, that the DSM is a mean-field model, so the stress tensor of the system is a sum of the stresses of its individual molecular components

$$\tau = \sum_{\gamma=1}^{n_m} \tau_\gamma. \tag{13}$$

6

The stress tensor of a component is found from thermodynamics [21, 16]

$$\tau_\gamma(t) = -n_\gamma \left\langle \sum_{i=2}^{Z-1} \boldsymbol{Q}_i \left(\frac{\partial F(\Omega)}{\partial \boldsymbol{Q}_i} \right)_{T,\{N_i\},\boldsymbol{Q}_{k\neq i}} \right\rangle_\gamma, \tag{14}$$

where $\langle ... \rangle_\gamma$ is an average over the γth component. Using equations (12–14) we calculate the relaxation modulus of the system to be

$$G(t) = \sum_{\gamma=1}^{n_m} w_\gamma G_\gamma(t), \tag{15}$$

where $G_\gamma(t)$ is the relaxation modulus of the γth component in the system.

To obtain the dynamic modulus, $G^*(\omega)$, we fit a relaxation spectrum, $h_\gamma(\tau)$, to $G_\gamma(t)$

$$G_\gamma(t) = G^0_{N,\gamma} \int_0^\infty \frac{h_\gamma(\tau)}{\tau} \exp\left(-\frac{t}{\tau}\right) d\tau. \tag{16}$$

We find that $h_\gamma(\tau)$ represented by a BSW spectrum [1] describes model predictions very well

$$h_\gamma(\tau) = \sum_{k=1}^{l_\gamma} \frac{g_{k,\gamma} \alpha_{k,\gamma} \tau^{\alpha_{k,\gamma}} H(\tau^{\max}_{k,\gamma} - \tau) H(\tau - \tau^0_{k,\gamma})}{\left(\tau^{\max}_{k,\gamma}\right)^{\alpha_{k,\gamma}} - \left(\tau^0_{k,\gamma}\right)^{\alpha_{k,\gamma}}}, \tag{17}$$

where $g_{k,\gamma}$, $\alpha_{k,\gamma}$, $\tau^0_{k,\gamma}$, $\tau^{\max}_{k,\gamma}$ are the fitting parameters and l_γ is the number of fitting modes for the γ component. We find that $l_\gamma = 1$ is enough for the low-molecular-weight component, and $l_\gamma = 2$ for the high-molecular-weight component in bidisperse blends.

The dynamic moduli, $G^*_\gamma(\omega)$, are calculated analytically from the one-sided Fourier transform of eq.(16) multiplied by $i\omega$. The expressions for $G'_\gamma(\omega)$ and $G''_\gamma(\omega)$ are

$$
\begin{aligned}
G'_\gamma(\omega) &= G^0_{N,\gamma}\omega^2 \sum_{i=1}^m \frac{\prod_{j=0}^{i-1} \tau_j^{\alpha_j - \alpha_{j+1}}}{\alpha_i + 2} \left[{}_2F_1\left(1, \frac{\alpha_i+2}{2}; \frac{\alpha_i+4}{2}; -\omega^2\tau_i^2\right) \tau_i^{\alpha_i+2} - \right.\\
&\quad \left. {}_2F_1\left(1, \frac{\alpha_i+2}{2}; \frac{\alpha_i+4}{2}; -\omega^2\tau_{i-1}^2\right) \tau_{i-1}^{\alpha_i+2} \right] / \\
&\quad \sum_{i=1}^m \frac{\prod_{j=0}^{i-1} \tau_j^{\alpha_j - \alpha_{j+1}} \left(\tau_i^{\alpha_i} - \tau_{i-1}^{\alpha_i}\right)}{\alpha_i}
\end{aligned} \tag{18}
$$

$$
\begin{aligned}
G''_\gamma(\omega) &= G^0_{N,\gamma}\omega \sum_{i=1}^m \frac{\prod_{j=0}^{i-1} \tau_j^{\alpha_j - \alpha_{j+1}}}{\alpha_i + 1} \left[{}_2F_1\left(1, \frac{\alpha_i+1}{2}; \frac{\alpha_i+3}{2}; -\omega^2\tau_i^2\right) \tau_i^{\alpha_i+1} - \right.\\
&\quad \left. {}_2F_1\left(1, \frac{\alpha_i+1}{2}; \frac{\alpha_i+3}{2}; -\omega^2\tau_{i-1}^2\right) \tau_{i-1}^{\alpha_i+1} \right] / \\
&\quad \sum_{i=1}^m \frac{\prod_{j=0}^{i-1} \tau_j^{\alpha_j - \alpha_{j+1}} \left(\tau_i^{\alpha_i} - \tau_{i-1}^{\alpha_i}\right)}{\alpha_i},
\end{aligned} \tag{19}
$$

7

where $_2F_1(a, b, c, d)$ is the hypergeometric function. Using equations 15, 18 and 19 we calculate the dynamic modulus of the polydisperse blend.

Calculations with the model may now be compared with experiments. There are only three parameters, the first of which is known *a priori* from static light scattering experiments: M_K, the molecular weight of a Kuhn step, β, the average number of Kuhn steps between entanglements minus one, and τ_K the characteristic time for a Kuhn step to move through an entanglement. The second parameter determines the height of the plateau modulus for very high molecular weights, and the last determines all time scales. They are independent of molecular weight and can be fit to a single monodisperse system.

Figure 1 shows a typical comparison for two monodisperse polystyrene melts, and a blend of 20% by volume blend of high molecular weight for the dynamic modulus. We note that the model does not agree at the highest frequencies because these rapid dynamics have been purposefully coarse-grained out. Secondly, we see that the smallest molecular weight data relax somewhat more slowly than predicted by the theory. However, these chains are barely entangled ($\langle Z \rangle_{eq} \cong 3$), whereas the theory assumes that entanglements are the dominate mechanism where stress resides. Hence, the theory is expected to break down at these low molecular weights. The theory is able to describe the high-molecular-weight data very well, but there may be some effects of polydispersity ignored in the calculations. Finally we note that the theory is indeed able to describe the blend of the two molecular weights. We called these results 'typical', although much better agreement is seen when the above limitations of entanglement number and polydispersity are avoided in the data.

2.1.2 Cross-linked polymer rheology predictions

The results in this section are from [11]. The implementation of the theory is very similar to that of the previous section. However, now we have two different kinds of strands: entangled network strands, and dangling ends. These are sketched in Figure 2.

Experiments were performed elsewhere [7, 6] on chains that are end-functionalized and monodisperse. While such systems are more ideal, polydispersity still arises during cross-linking. For example, entangled network strands could still have an integer number of chains. Or, loops and dangling ends of complicated structures can arise. In real system, it is difficult to know the exact distribution of such structures. In this work we considered only monodisperse network strands, and two possibilities for linear dangling ends.

The procedure for handling constraint dynamics is very similar. However, the details are different. First, some entanglements are permanently trapped, so have a characteristic lifetime that is infinity. Dangling ends have lifetimes that are very similar to linear melts at short times, but then live longer, because there is only one end to relax entanglements. The former observation is illustrated in Figure 3, which shows the survival function of entanglements for a dangling end—a chain with one end attached permanently to the network, but the other is free. Also shown for comparison is the survival of linear chain of the same
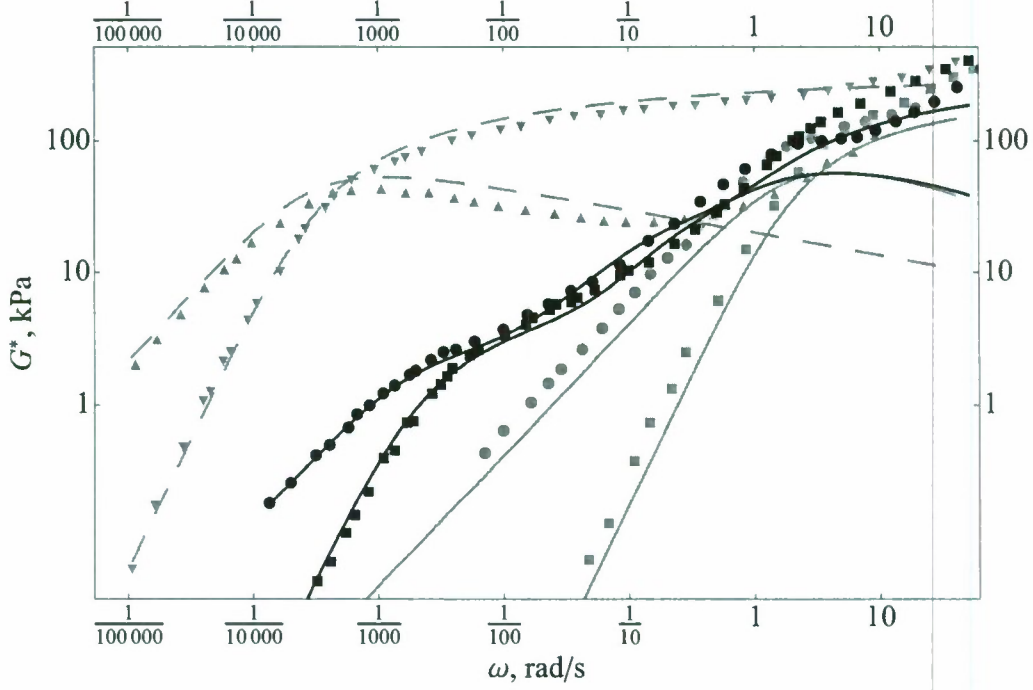
8

Figure 1: Comparison of the DSM LVE predictions with experimental data by Watanabe et al. Gray symbols and black triangles are experimental data for PS39 and PS427, black squares and circles are bidisperse mixture PS39&427 [24]. Lines are the DSM predictions.

molecular weight in the melt. The curves are spectra fitted to the expression

$$
\begin{aligned}
p^{CD}(\tau) &= w_{DS}\left(\frac{\tau^{\alpha_1-1}H(\tau-\tau_0)H(\tau_1-\tau)}{\frac{\tau_1^{\alpha_1}-\tau_0^{\alpha_1}}{\alpha_1}+\frac{\tau_2^{\alpha_2}-\tau_1^{\alpha_2}}{\alpha_2}\tau_1^{\alpha_1-\alpha_2}}+\frac{\tau^{\alpha_2-1}H(\tau-\tau_1)H(\tau_2-\tau)\tau_1^{\alpha_1-\alpha_2}}{\frac{\tau_1^{\alpha_1}-\tau_0^{\alpha_1}}{\alpha_1}+\frac{\tau_2^{\alpha_2}-\tau_1^{\alpha_2}}{\alpha_2}\tau_1^{\alpha_1-\alpha_2}}\right)\\
&+ w_{NS}\frac{2\delta(1/\tau)}{\tau^2}.
\end{aligned}
\tag{20}
$$

where the last term is for the permanently trapped entanglements, and

$$
\begin{aligned}
f_d(t) &= 1-\mathbb{P}(t)\\
&= \frac{\int_0^\infty \frac{p^{CD}(\tau^{CD})}{\tau^{CD}}\exp\left(-\frac{t}{\tau^{CD}}\right)d\tau^{CD}}{\int_0^\infty \frac{p^{CD}(\tau^{CD})}{\tau^{CD}}d\tau^{CD}}\\
&= \frac{\int_0^\infty \frac{p_{DS}^{CD}(\tau^{CD})}{\tau^{CD}}\exp\left(-\frac{t}{\tau^{CD}}\right)d\tau^{CD}}{\int_0^\infty \frac{p_{DS}^{CD}(\tau^{CD})}{\tau^{CD}}d\tau^{CD}},
\end{aligned}
\tag{21}
$$

These expressions are used to carry around detailed information efficiently about the self-consistent lifetime distributions from constraint dynamics. They introduce no adjustable parameters, since all constants in eqn. (20) are found from sliding dynamics calculations.
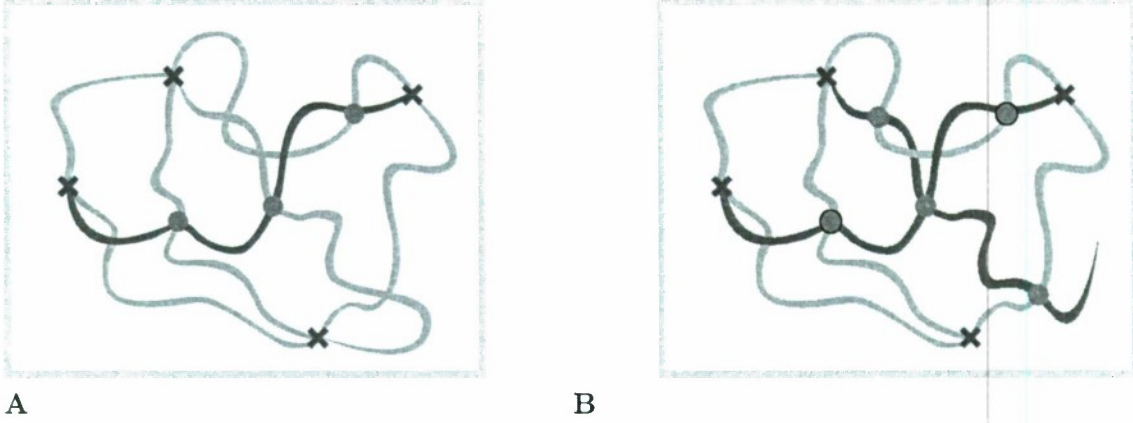
9

Figure 2: A: Drawing of an ideal entangled network (IEN). All cross-linking points are reacted and no dangling ends, are present. The cross-linkers are represented as discrete points (black crosses) and gray circles are marking the trapped entanglements. B: Illustration of a network with elastic active network strands and a dangling strand. Gray circles mark entanglements, where the trapped have been marked additionally with black rings. The cross-linking points are considered as discrete points and marked as black crosses.
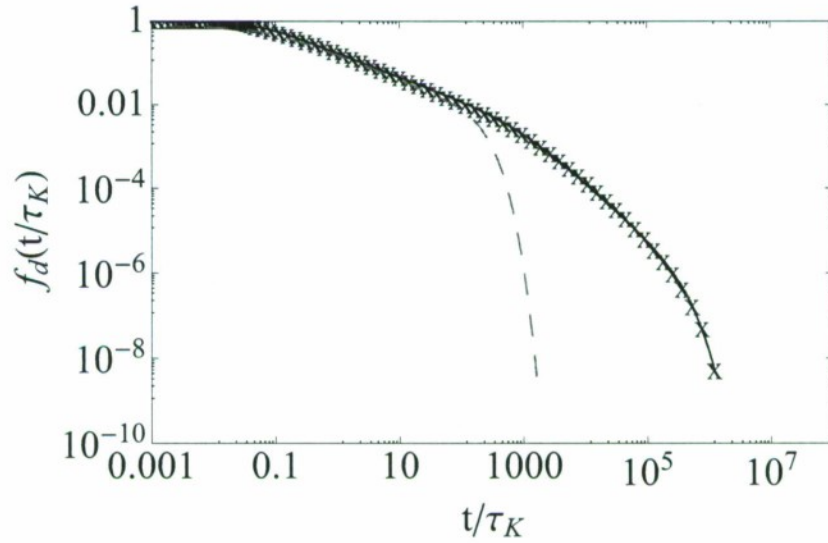

Figure 3: $f_d(t)$ obtained from a simulation of the EDS model with $N_K = 60$ and $\beta = 20$ and an ensemble of 100 chains. The crosses are simulated data, while the full line is a fitted spectrum: $\tau_0 = 0.0498, \tau_1 = 1151, \tau_2 = 264451, \alpha_1 = 0.453$ and $\alpha_2 = -0.271$. The dashed red line is $f_d(t)$ for linear chains with the same N_K and β.

10

2.2 A progressive coarse graining of the theory to create a continuum-level description.

The more-common theoretical approach for entangled polymers, called "tube models" is based on the Doi-Edwards tube theory. While it is typically computationally easier than the slip-link model, and is sometimes able to show good quantitative agreement with data, it does suffer some drawbacks. First, it is not a single mathematical model. Rather, there exist completely different mathematical objects depending on chain architecture, whether one considers only linear viscoelasticity or flow, or if there are blends. Even those models that show promise in nonlinear rheology, are expected to have problems in reversing deformations. Secondly, there is not a strong connection between tube models and statistical mechanics, or thermodynamics. As a result, it is difficult to make connections to molecular-level simulations, or to be certain that instabilities might not arise in certain deformations.

In this work, we seek to derive continuum models on a level with existing tube models, but are strongly tied to the slip-link model. In this way, we might have a spectrum of mathematical models that are connected, but could be used where appropriate. Also, one can more easily make controlled approximations with some certainty on where to pin the blame when there is a failure comparing to experiments. To date, we have accomplished two important steps towards this goal. Comparison with atomistic simulations suggested that the model required some generalization regarding entanglement motion. This generalization also made the model closer in spirit to tube models. The first step was the generalization to consider mobile slip-links, and the second step was smooth out the discrete parts of the free energy so that it might be used to derive a continuum model. The first work was published in the *Journal of Chemical Physics*, while the second will be submitted very soon (to the same journal).

2.2.1 Mobile slip-links

In the slip-link model described so far, the entanglements are treated as point objects, fixed in space or deforming affinely with the macroscopic flow. In reality of course, the effects of entanglements allow some fluctuations. As a result, Likhtman's slip-spring simulation [13] allows the position of the entanglements to fluctuate around a fixed point using virtual springs. However, such an implementation raises questions about the proper expression for the stress tensor, and how it can be made thermodynamically consistent. For example, Likhtman has proposed two different expressions for stress, and it is not yet clear whether either of these is correct. We recently modified the slip-link model to allow such fluctuations [20], but utilized ideas from Rubenstein and Panyukov [19] to remove the contributions of the virtual springs to the stress tensor. We only mention the conclusions of that paper here, that we find that the static properties and stress-tensor expression of the model are largely unchanged, and that thermodynamic consistency can be recovered.

11

2.2.2 Free energy expressions for tube models

Using some of the results from the paper of the previous section [20], we have derived a free energy for a slip-link model that is more like a tube model. In fact, the expression reduces to a free energy [17] that is used to justify the GLaMM tube model [5].

We find an expression for the free energy of an entangled chain, where the entanglements are no longer discrete points, but rather are smeared out along the primitive path. Moreover, these are allowed to fluctuate around the mean path. These fluctuations introduce a new parameter n, which characterizes their strength. However, we find that its value is easily estimated from the primitive path analysis of atomistic simulations [3, 22, 4, 8], so it is not adjusted

$$\frac{F[\hat{\Omega}_{c,e}]}{k_B T} = \frac{3}{2} \int_0^Z \left\{ \frac{\hat{Q}(i)^2}{N(i)a_K^2} + \frac{n}{a_K^2} \left[\frac{d}{di} \left(\frac{\hat{Q}(i)}{N(i)} \right) \right]^2 + 2 \log N(i) \right\} di$$
$$- \frac{3}{2} \log \left[\left(\frac{3n}{2\pi a_K^2} \right)^Z s_{[0,Z]}(Z) \right]. \tag{22}$$

Note that the quantity $s_{[0,Z]}$ is found from the ODE

$$\frac{d^2 s_{[0,Z]}}{di^2} = \frac{N(i)}{n} s_{[0,Z]}(i) \tag{23}$$

with the boundary conditions

$$s_{[0,Z]}(0) = 1, \tag{24}$$

$$\left. \frac{ds_{[0,Z]}}{di} \right|_{i=0} = \frac{N(0)}{2n} + 1 \tag{25}$$

Here, the variables $\{\hat{Q}_i\}$ are the mean positions of the primitive path. KampWe also found the resulting chemical potential μ,

$$\frac{\mu(i)}{k_B T} = \frac{1}{k_B T} \left(\frac{\delta F[\hat{\Omega}_{c,e}]}{\delta N(i)} \right)_{T,Z,\hat{Q}(i)}$$
$$= -\frac{3\hat{Q}(i)^2}{2N(i)^2 a_K^2} + \frac{3n\hat{Q}(i)}{N(i)^2 a_K^2} \cdot \frac{d^2}{di^2} \left(\frac{\hat{Q}(i)}{N(i)} \right) + \frac{3}{N(i)}$$
$$- \frac{3}{2s_{[0,Z]}(Z)} \left(\frac{\delta s_{[0,Z]}(Z)}{\delta N(i)} \right)_{T,Z,\hat{Q}(i)}, \tag{26}$$

and the stress tensor τ

$$\tau = -\frac{3n_c k_B T}{a_K^2} \left\langle \int_0^Z \left[\frac{\hat{Q}(i)\hat{Q}(i)}{N(i)} + n \frac{d}{di} \left(\frac{\hat{Q}(i)}{N(i)} \right) \frac{d}{di} \left(\frac{\hat{Q}(i)}{N(i)} \right) \right] di \right\rangle. \tag{27}$$

Note that this expression has not yet exploited the ideas of Rubenstein and Panyukov, because of the presence of the second term on the right side. However, judiciously chosen dynamics of the virtual springs can be used to cancel this term.

This work will be submitted for publication very shortly.

2.3 Make available to the Army resulting computer code.

We have made available to ARL several codes to date. Two of these were were created in our lab, and one in the lab of Martin Kröger of ETH. The first is the discrete slip-link model described in some detail above. However, it can be used predict nonlinear flows, and not just the dynamic modulus G^*. Secondly, since we saw that are model gives results similar to the GLaMM model (but with fewer parameters), and that our coarse-graining efforts of the DSM were moving in a similar direction, we also coded a numerical simulation of the GLaMM model, and provided it to MMB at ARL. This code runs much faster than that necessary to make accurate calculations of the DSM. Thirdly, we provided the Z1 code of Martin Kröger [12], which can be used for primitive path analysis.

2.4 Generalization to co-polymers.

We expended considerable effort to correct the problems of thermodynamics in the primitive chain network (PCN) simulations of Yuichi Masubuchi. We hosted for several months his graduate student, Kazushi Horio, and made detailed derivations of a proper free-energy expression. However, before we completed that work, Mr. Horio was pulled off of that project and on to experimental work in the lab of the senior professor at Kyoto University. While those derivations are finished, there has been no computer code yet written to incorporate the results. Once written, the approach could be used in a straightforward way to incorporate blends of monomer chemistry. The approach would be something like a hybrid of the slip-link model and seld-consisten field theory.

To resurrect that work, we have begun collaborations with Prof. Juan de Pablo at the University of Wisconsin. He has already successfully created new technology to make self-consistent field theory calculations very efficiently. We have been adding dynamics and entanglements to the code through slip-link ideas. A manuscript is currently in preparation.

2.5 Generalization to semi-flexible polymers.

In order to generalize the theory for biological systems, such as actin filament networks in the cytoskeleton, we need to find the free energy for a semi-flexible chain. The work above massively exploits the fact that the persistence length of a chain is the smallest length scale. In fact, one finds that the persistence length can be eliminated from the equations for stress completely. Also, the free energy for the chain can be written as the sum of the independent free energies of all the entangled strands.

Determination of the free energy of a semi-flexible chain with entanglement constraints is a well-posed, straightforward question of statistical mechanics. However, the calculations are nontrivial. Work in this direction was begun by Yamakawa [25], but a great leap forward was recently made by Andrew Spakowitz and coworkers at Stanford University [15]. Therefore we began collaborating with Prof. Spakowitz to complete the statistical mechanical calculations for our problem. The derivation is rather lengthy, and not yet complete. However, we have overcome most obstacles to find the necessary Green's function for a semi-flexible chain with

13

Z strands ($Z-1$ entanglements), whose ends are free to fluctuate

$$
\begin{aligned}
G(\boldsymbol{R}, L) \;=\; & \frac{1}{\pi} \int \sum_{l_0=0}^{\infty} \mathcal{G}_{l_0}^{0,0}(k; L_1) j_{l_0}(-k Q_1) k^2 \mathrm{d}k \\
& \int \sum_{l_z=0}^{\infty} \mathcal{G}_{0}^{l_z,0}(k; L_Z) j_{l_z}(-k Q_Z) k^2 \mathrm{d}k \\
& \prod_{j=2}^{Z-1} \int \sum_{l_1=0}^{\infty} \sum_{l_2=0}^{\infty} \sum_{m=-\min(l_1,l_2)}^{\min(l_1,l_2)} \mathcal{G}_{l_1}^{l_2,m}(k; L_j) \sum_{n=|l_1-l_2|}^{l_1+l_2} j_n(-k Q_j) i^n (-1)^m \\
& \langle l_1 0 l_2 0 | n 0 \rangle \langle l_1 m l_2 -m | n 0 \rangle k^2 \mathrm{d}k
\end{aligned}
$$

where

$$
\mathcal{G}_{l_0}^{l_f,m}(k; L) \;=\; \sum_{i=0}^{\infty} \frac{e^{\mathcal{E}_i L}}{\partial_p J(p)_{p=\mathcal{E}_i}}, \tag{28}
$$

and J is the poles of a function determined by a recursion formula, j_n are spherical Bessel functions, and the angular brackets represent Clebsch-Gordan coefficients. The point here is that this expression would clearly be computationally prohibitive for predictions. So, we are currently performing calculations of the exact result to search for useful approximations of the free energy.

3   Bibliography

References

[1] M. Baumgaertel, A. Schausberger, and H.H. Winter. The relaxation of polymers with linear flexible chains of uniform length. *Rheologica Acta*, 29(5):400–408, 1990.

[2] M. Doi and J.-I. Takimoto. Molecular modelling of entanglement. *Royal Society of London Philosophical Transactions Series A*, 361:641–652, April 2003.

[3] Ralf Everaers, Sathish K. Sukumaran, Gary S. Grest, Carsten Svaneborg, Arvind Sivasubramanian, and Kurt Kremer. Rheology and microscopic topology of entangled polymeric liquids. *Science*, 303:823–826, 2004.

[4] K. Foteinopoulou, N.Ch. Karayiannis, V.G. Mavrantzas, and M. Kröger. Primitive path identification and entanglement statistics in polymer melts: Results from direct topological analysis on atomistic polyethylene models. *Macromolecules*, 39(12):4207–4216, 2006.

[5] Richard S. Graham, Alexei Likhtman, Tom C. B. McLeish, and Scott T. Milner. Microscopic theory of linear, entangled polymer chains under rapid deformation including chain stretch and convective constraint release. *J. Rheol.*, 47(5):1171–1200, September/October 2003.

[6] Mette Jensen, Ole Hassager, Henrik Rasmussen, Anne Skov, Anders Bach, and Henning Koldbech. Planar elongation of soft polymeric networks. *Rheologica Acta*, 49:1–13, 2010. 10.1007/s00397-009-0383-7.

[7] Mette Jensen, Henrik Rasmussen, Anne Skov, and Ole Hassager. Reversed planar elongation of soft polymeric networks. *Rheologica Acta*, 50:729–740, 2011. 10.1007/s00397-011-0552-3.

[8] R. N. Khaliullin and J. D. Schieber. Analytic expressions for the statistics of the primitive-path length in entangled polymers. *Physical Review Letters*, 100(18):188302, May 2008.

[9] Renat N. Khaliullin and Jay D. Schieber. Application of the slip-link model to bidisperse systems. *Macromolecules*, 43(14):6202–6212, 2010.

[10] R.N. Khaliullin and J.D. Schieber. Self-consistent modeling of constraint release in a single-chain mean-field slip-link model. *Macromolecules*, 42(19):7504–7517, October 2009.

[11] Mette Krog Jensen, R. N. Khaliullin, and Jay D. Schieber. Self-consistent modeling of entangled network strands and dangling ends. *Rheological Acta*, pages 0035–4511, 2011. in press.

[12] Martin Kröger. Shortest multiple disconnected path for the analysis of entanglements in two- and three-dimensional polymeric systems. *Computer Physics Communications*, 168(3):209–232, June 2005.

[13] A.E. Likhtman. Single-chain slip-link model of entangled polymers: Simultaneous description of neutron spin-echo, rheology, and diffusion. *Macromolecules*, 38(14):6128–6139, 2005.

[14] AE Likhtman and TCB McLeish. Quantitative theory for linear dynamics of linear entangled polymers. *Macromolecules*, 35(16):6332–6343, 2002.

[15] Shafigh Mehraeen, Bariz Sudhanshu, Elena F. Koslover, and Andrew J. Spakowitz. End-to-end distribution for a wormlike chain in arbitrary dimensions. *Physical Review E (Statistical, Nonlinear, and Soft Matter Physics)*, 77(6):061803, 2008.

[16] D. M. Nair and J. D. Schieber. Linear viscoelastic predictions of a consistently unconstrained brownian slip-link model. *Macromolecules*, 39(9):3386–3397, May 2006.

[17] D. J. Read, K. Jagannathan, and A. E. Likhtman. Entangled polymers: constraint release, mean paths, and tube bending energy. *Macromolecules*, 41:6843–6853, 2008.

[18] M. Rubinstein and R.H. Colby. Self-consistent theory of polydisperse entangled polymers: Linear viscoelasticity of binary blends. *Journal of Chemical Physics*, 89(8):5291–, October 1988.

[19] Michael Rubinstein and Sergei Panyukov. Elasticity of polymer networks. *Macromolecules*, 35(17):6670–6686, 2002.

[20] Jay Schieber and Kazushi Horio. Fluctuation in entanglement positions via elastic slip-links. *Journal of Chemical Physics*, 132:074905, 2010.

[21] Jay D. Schieber. Fluctuations in entanglements of polymer liquids. *The Journal of Chemical Physics*, 118(11):5162–5166, 2003.

[22] Christos Tzoumanekas and Doros N. Theodorou. Topological analysis of linear polymer melts: A statistical approach. *Macromolecules*, 39(13):4592–4604, 2006.

[23] Nico G. van Kampen. *Stochastic Processes in Physics and Chemistry*. North-Holland, Amsterdam, 1992.

[24] Watanabe. Viscoelastic properties and relaxation mechanisms of binary blends of narrow molecular weight distribution polystyrenes. *Macromolecules*, 1984.

[25] Hiromi Yamakawa. *Modern theory of polymer solutions*. Harper and Row, New York, 1971. Available online as pdf file at http://www.molsci.polym.kyoto-u.ac.jp/archives/redbook.pdf.